Biochar (2021) 3:469–484
https://doi.org/10.1007/s42773-021-00112-3

ORIGINAL RESEARCH

Effect of pyrolysis temperature on Si release of alkali-enhanced Si-rich biochar and plant response

Meng Wang[1,2,3] · Negar D. Tafti[2] · Jim J. Wang[2] · Xudong Wang[3]

Received: 23 March 2021 / Accepted: 1 July 2021 / Published online: 27 July 2021

Abstract

Recent studies have shown that silicon (Si) dissolution from biochar may be influenced by the pyrolysis temperature. In addition, the enhancement of biochar by treatment with alkali has been proposed to produce a Si source that can be used for environmentally friendly plant disease control. In this study, biochars from rice straw and rice husk pretreated with KOH, CaO and K_2CO_3 and then pyrolyzed at 350, 450 and 550 °C were prepared to evaluate the effects of pyrolysis temperature on Si release and plant uptake from alkali-enhanced Si-rich biochar. Extractable Si and dissolution Si from the prepared biochars were assessed by different short-term chemical methods and long-term (30-day) release in dilute acid and neutral salt solutions, respectively, along with a rice potting experiment in greenhouse. For both rice straw- and husk-derived alkali-enhanced biochars (RS-10KB and HS-10K2B, respectively), increasing the pyrolysis temperature from 350 to 550 °C generally had the highest extractable Si and increased Si content extracted by 5-day sodium carbonate and ammonium nitrate (5dSCAN) designated for fertilizer Si by 61–142%, whereas non-enhanced biochars had more extractable Si at 350 °C. The alkali-enhanced biochars produced at 550 °C pyrolysis temperature also released 82–172% and 27–79% more Si than that of 350 °C produced biochar in unbuffered weak acid and neutral salt solutions, respectively, over 30 days. In addition, alkali-enhanced biochars, especially that derived from rice husk at 550 °C facilitated 6–21% greater Si uptake by rice and 44–101% higher rice grain yields than lower temperature biochars, non-enhanced biochars, or conventional Si fertilizers (wollastonite and silicate calcium slag). Overall, this study demonstrated that 550 °C is more efficient than lower pyrolysis temperature for preparing alkali-enhanced biochar to improve Si release for plant growth.

Keywords Silicon · Biochar · Extractable Si · Si release · Plant uptake

1 Introduction

The beneficial effect of Si on plant growth has been well documented. It includes improving plant resistance to pest and disease, enhancing mechanical strength, and decreasing nutrient imbalance, as well as alleviating metal toxicity and other stresses due to soil salinity, extreme temperature and drought conditions (Meyer and Keeping 2001; Neumann and Zur 2001; Epstein 2009; Guntzer et al. 2012; Adrees et al. 2015; Islam et al. 2020). Thus, the application of Si fertilizers to plants, especially Si-accumulators such as rice, maize, sugarcane, wheat, and ryegrass is necessary to ensure plant healthy growth. Recently, several studies have shown that biochars produced by pyrolyzing Si-rich waste biomass could be also used as bioavailable Si source to Si-accumulator plants (Houben et al. 2014; Liu et al. 2014; Li et al. 2014, 2018; Abbas et al. 2017; Linam et al. 2021). Application of biochars significantly increased Si content in stem and blades of wheat, rice, and perennial ryegrass (Liu et al. 2014; Abbas et al. 2017; Wang et al. 2018a, 2019a). Therefore, biochar could serve as a low-cost, renewable, and environmentally friendly Si source.

The characteristics of biochar are influenced by various factors, including feedstock biomass types and pyrolysis conditions. Pyrolysis temperature has been considered as

✉ Jim J. Wang
jjwang@agcenter.lsu.edu

1 College of Chemical and Environment Science, Shaanxi University of Technology, Hanzhong, Shaanxi 723001, China

2 School of Plant, Environmental and Soil Science, Louisiana State University, 104 Sturgis Hall, Baton Rouge, LA 70803, USA

3 College of Natural Resources and Environment, Northwest A&F University, Yangling, Shaanxi 712100, China

one of the most important factors affecting physical, chemical and structural characteristics of biochar (Singh et al. 2012; Keiluweit et al. 2010; Nguyen et al. 2010; Kuzyakov et al. 2009). Compared with biochars prepared at low temperatures, high-pyrolysis temperature biochars tend to have higher carbon content, pH, ash content, specific surface area, aromatization and thermal stability, but exhibit lower nitrogen content, yield, and aliphatic carbon fractions (Huang et al. 2020; Suliman et al. 2016; Ahmad et al. 2012; Kim et al. 2012; Novak et al. 2009).

Pyrolysis temperature also affects the interaction of carbon with silicon in biochar. For biomass feedstocks that are rich in amorphous silicon, it was reported that pyrolysis in the temperature range of 250 ~ 350 °C could cause a crack of carbon layer in the C–Si–C structural configuration of biomass which exposes internal Si and leads to an increasing solubility of Si in biochar (Xiao et al. 2014). However, as pyrolysis temperature is further raised to 500 ~ 700 °C, the solubility of Si is decreased due to aromatization of carbon and formation of more crystallized silica (Xiao et al. 2014). On the other hand, a new study reported generally continuous increase in accumulative Si dissolution from several biochars derived from both Si-rich and deficient biomass feedstocks as pyrolysis temperature increased from 300 to 700 °C (Wang et al. 2018b). While Si release rates for Si-rich biochars were found to be similar at different pyrolysis temperatures with different final amounts of total Si released, the Si-deficient biochars showed a high and low stages of Si release rates but with no difference in the final amount of total Si dissolved (Wang et al. 2018b). In addition, others also reported the increasing extractable Si content of rice husk and sugarcane bagasse biochars based on chemical extractions as pyrolysis temperature increased from 300 to 700 °C (Nwajiaku et al. 2018). These results suggest the solubility of Si or Si availability of biochar likely depends on the interaction between the specific feedstock and pyrolysis temperature. These biochar Si solubility characteristics have not been evaluated in regard to plant response. On the other hand, Wang et al. (2018a,2019a) recently proposed the use of alkali-enhanced biochar as Si fertilizer. However, the effects of pyrolysis temperature on the properties of alkali-enhanced biochars have not yet been explored.

In this study, rice straw and husk were selected to prepare KOH, K_2CO_3 and CaO-enhanced Si-biochars at different pyrolysis temperatures. The effects of temperature on physical and chemical properties as well as total and extractable Si were investigated. In addition, since the dissolution tendency of Si in Si fertilizer was highly correlated with Si content released into soil (Korndörfer et al. 2001; Sebastian et al. 2013; Xiao et al. 2014), soil available Si for crop absorption could be simulated by acid or alkali extraction due to depolymerization of non-monomeric Si (Iler 1979; NIAES 1987; Bao 2000). Moreover, soil pH changes could affect biochar phytolith Si dissolution (Fraysse et al. 2006; Wang et al. 2018a). Therefore, weak acid and neutral salt solution were chosen to evaluate Si release of alkali-enhanced biochars prepared at different pyrolysis temperatures, and the associated plant response was measured to provide a basis for the rational application of alkali-enhanced biochar as an alternative Si source.

2 Materials and methods

2.1 Alkali-enhanced biochar preparation

Rice straw (RS) and husk (RH) collected from Louisiana State University AgCenter Rice Research Station (Crowley, LA, USA) were utilized for biochar preparation. Collected feedstock samples were rinsed using deionized (D.I.) water and then dried at 60 °C for 24 h. The dried rice straw and husk biomass samples were ground to pass a 1-mm sieve using a cutting mill. For making biochar, rice straw and husk were mixed, respectively, with KOH, K_2CO_3 or CaO, in powder form and at alkali:biomass ratios (on weight basis) of 0:100, 5:100, and 10:100 in a porcelain crucible followed by mixing with 100 mL of D.I. water (for 50 g biomass) for 90 min. The biomass-containing crucibles were then placed in muffle furnace under N_2 flow at 400 mL min^{-1} to purge air from the system for 30 min. Pyrolysis was carried out by setting muffle furnace temperature at 180 °C for dehydration for 30 min and then maintaining at 350, 450 and 550 °C, respectively, for 60 min under N_2 purge at 200 mL min^{-1} (Wang et al. 2018a). The resulting biochar samples were cooled and ground to pass a 1-mm sieve before characterization. For convenience of discussion, these produced biochars are referred as 0B (no alkali pretreatment), 5KB and 10KB (pretreatment with KOH at 5:100 and 10:100 ratio), 5K2B and 10K2B (pretreatment with K_2CO_3 at 5:100 and 10:100 ratio), and 5CB and 10CB (pretreatment with CaO at 5:100 and 10:100 ratio), respectively.

2.2 Chemical characterization of biochar Si and its release

Biochar sample pH was measured based on 1:100 biochar to D.I. water ratio (Cantrell et al. 2011). Ash content was measured by furnace at 550 °C for 5 h. Total C and N analyses were carried out using an elemental analyzer (Elementar Analysen systeme GmbH, Germany). Biochar total P, K, Ca, Mg, Cu and Fe were determined by ICP-AES (SPECTRO Plasma 3200, Germany) after digestion with nitric acid and H_2O_2 (Huang and Schulte 1985). Total Si in alkali-enhanced biochars and feedstocks was determined using a 1.5 M HF–0.6 M HCl extraction, and fertilizer soluble Si fraction in biochar samples was evaluated using 5-day sodium

carbonate and ammonium nitrate (Na_2CO_3–NH_4NO_3) extraction (referred as 5dSCAN) designated by the Association of American Plant Food Control Officials (AAPFCO) followed by light absorption spectrometry (Saito et al. 2005; Sebastian et al. 2013). Specifically, the HF–HCl extraction was performed at a 1:100 solid to solution ratio for 1 h with stirring every 10 min**.** The 5dSCAN extraction procedure was carried out at a 1:1000 solid to solution ratio for 1 h shaking (at 140 rpm) followed by settling for 4 days and 23 h. The samples were then filtered using a Whatman filter paper (< 2.5µ) before Si analysis.

Four additional Si test methods including 0.5 M HCl, 1 M sodium acetate buffer (pH 4.0), 1-h equilibrium of 0.094 M Na_2CO_3–0.2 M NH_4NO_3 mixed solution (1hSCAN), and 0.5 M ammonium acetate were also used to determine different levels of extractable Si from alkali-enhanced biochars along with commonly used mineral Si fertilizer wollastonite (WO) (W10, Vansil®, R.T. Vanderbilt Co, Norwalk, CT). Among these four methods, 0.5 M HCl is the official procedure to evaluate available Si from slag-based calcium silicate fertilizer in Japan (NIAES 1987; Ma and Takahashi 2002). The 1 M acetate buffer (pH 4.0) method is widely used to evaluate available Si in soil as well as in slags (NIAES 1987). The method could extract soluble and some exchangeable Si (Snyder 2001), although it has been shown to over-estimate Si availability in soil amended with calcium silicate slag (Takahashi 1981) and in calcareous soils (Liang et al. 1994). The 0.5 M ammonium acetate extraction method also extracts soluble and some exchangeable Si (Takahashi 1981; Kato and Owa 1997). The 1hSCAN extraction, the shorter version of 5dSCAN procedure, has been routinely used in Brazil (Korndorfer et al. 2004). For these four methods, the extractions were based on 1:1000 solid to solution ratio for 1 h of shaking at 140 rpm followed by filtration (Hallmark et al. 1982; Wang et al. 2004).

In addition, the total Si released during 30 days from RS, RH, K_2CO_3-enhanced RS and RH biochars (RS-0B/5K2B/10K2B and RH-0B/5K2B/10K2B) was evaluated in unbuffered weak acid solution (0.1 mM HCl) and neutral salt solution (0.01 M KCl), respectively. For comparison, wollastonite (WO) and industrial by-product silicate slag (SL) (SILI-CAL™, Calcium Silicate Corp., Lake Harbor, FL) samples were also investigated. In doing so, a series of 30-mg samples (ground to pass a 1-mm sieve) with each mixed with 30 ml of extractant solutions in 50-ml polyethylene centrifuge tubes were prepared. The mixtures were shaken continuously at 120 rpm under 25.0 ± 0.5 °C for 1 h, 1, 5, 9, 14, 21 and 30 days, respectively. The samples were then filtered using Whatman filter paper (< 2.5 µm) before analysis.

The Si in all the filtrates was determined using a SPECTRONIC 501 light absorption spectrophotometer (Thermo Scientific, Wilmington, DE) following blue silicomolybdous acid procedures (Hallmark et al. 1982; Wang et al. 2004; Sebastian et al. 2013). The spectrometer was calibrated using a standard curve for each extraction method before sample analysis. For all analytical procedures, duplicate samples were measured and a spike recovery of 95% of a known Si standard in selected samples was performed for quality control of analytical process.

2.3 Rice greenhouse potting study

A potting experiment using rice (*Oryza sativa* L) was conducted to assess plant response to the produced biochar Si source in the greenhouse at Louisiana State University, Baton Rouge, USA. The soil used in potting study was Crowley silt loam (fine-silty, montmorillonitic, thermic Typic Albaqualf) with pH 7.6, and its Mehlich-III soil-test extractable P and K were 10 and 69 mg kg^{-1}, respectively. Twelve types of Si sources including RS, RH, four alkali-enhanced RS biochars produced at 350 and 550 °C (RS-0B-350, RS-10K2B-350, RS-0B-550, RS-10K2B-550), four alkali-enhanced RH biochars produced at 350 and 550°C (RH-0B-350, RH-10K2B-350, RH-0B-550, RH-10K2B-550), WO, SL along with a control (CK) without addition of amendment were used. Each Si source was applied at the rate 0. 22% on soil mass basis (equivalent to 5 t ha^{-1}). All pots received a blanket application of N 0.0357 g kg^{-1} (80 kg N ha^{-1}), P_2O_5 0.0302 g kg^{-1} (68 kg P_2O_5 ha^{-1}), and K_2O 0.0302 g kg^{-1} (68 kg K_2O ha^{-1}) before planting. Two rice seeds were sown in a 12-cm diameter plastic pot. A second N application of 0.025 g kg^{-1} (56 kg ha^{-1}) was made to each pot after three weeks, and then the pot was flooded. Rice plants were harvested after 23 weeks of growth in the pots. Rice grain (husk and seed) and straw (stem and blade) were washed with deionized water and dried at 60 °C for 48 h. Plant Si content was analyzed by extracting the tissue with 1.5 M HF–0.6 M HCl, followed by detection using light absorption spectrometry (Saito et al. 2005; Sebastian et al. 2013). All treatments were replicated three times.

All statistical analyses were carried out using the Statistical Analysis Software, version 9.0 (SAS Institute, Cary, NC). Average results for the different treatments were compared using analysis of variance.

3 Results

3.1 Chemical and physical properties of alkali-enhanced biochars at different preparation temperatures

In general, biochar yield was reduced with increasing pyrolysis temperature in all alkali-enhanced biochars (Tables S1 and

S2). The pH and ash content of alkali-enhanced rice straw and husk biochars increased with increasing pyrolysis temperature (Tables S1 and S2). Specifically, the pH of 350 °C prepared RS-0B and RH-0B were 6.46 ~ 6.65, 450 and 550 °C treatments increased the pH of 0B by 1.53 ~ 2. 24 and 2.12 ~ 2.95 unit, respectively. As the proportion of KOH, K_2CO_3 and CaO increased, pH of biochars increased correspondingly. From 350 to 550 °C, ash contents of RS-0B and RH-0B increased from 32 and 34% to 45 and 44%, respectively. After alkali pretreatment, ash contents of 550 °C prepared rice straw- and husk-derived 10KB, 10K2B and 10CB were increased by 8 ~ 28%, 9 ~ 12% and 16 ~ 24%, respectively, as compared to non-enhanced 0B samples. Ash contents of 350 °C prepared biochars showed the similar trend.

The carbon content of both RS-0B and RH-0B biochar samples increased with increasing temperature while C and N contents decreased as alkali proportion increased (Tables S1 and S2). At 550 °C, C contents of 550 °C prepared RS- and RH-10KB, 10K2B, 10CB decreased by 22~24%, 7 ~ 11%, and 27 ~ 45%, respectively, comparing to 0B biochar samples. Increasing pyrolysis temperature also generally increased total P, K, Ca and Mg contents of RS and RH biochars, although they reached maximum concentrations at different temperature. As expected, biochar total K and Ca contents increased with increasing alkali amendment ratio of KOH, K_2CO_3 and CaO, respectively. Overall, all three alkali pretreatments affected the elemental composition of prepared biochars at different pyrolysis temperatures.

3.2 Total Si content of alkali-enhanced biochar at different preparation temperatures

Total Si in the alkali-enhanced biochar changed with biomass feedstock, pyrolysis temperature, and type and proportion of alkali pretreatment (Fig. 1). For 0B samples, total Si was maximized at 450 °C for rice straw and at 550 °C for rice husk. Increasing alkali pretreatment proportion tended to decrease total Si content in biochar samples with KOH, K_2CO_3 and CaO pretreatment. On the other hand, for the rice straw biochar, total Si content of 10KB prepared at 350 °C was 21.8% and decreased to 18.9% with increasing temperature. When pyrolysis temperature was raised to 550 °C, total Si content of 10CB was 64% higher than that of rice straw biochar prepared at 350 °C (Fig. 1A). A similar trend was also observed for rice husk biochars, although 0B samples had generally higher total Si compared to that of rice straw biochars (Fig. 1B), emphasizing the impact of the feedstock.

3.3 5dSCAN-extractable Si content of alkali-enhanced biochar at different preparation temperatures

Extractable Si evaluation of produced biochar Si sources using the designated 5dSCAN method by AAPFCO (Sebastian et al. 2013) for fertilizer Si is presented in Fig. 2. Although total Si was higher in rice husk biochar (Fig. 1), rice straw biochar showed generally higher 5dSCAN-Si (Fig. 2). For all pyrolysis temperatures, 5dSCAN-Si content of non-enhanced 0B samples, regardless of feedstock source, was higher than that of the feedstock sample. The non-enhanced 0B samples prepared at 350 °C exhibited the maximum Si content, but it decreased with pyrolysis temperature (Fig. 2). For biochar samples, increasing pyrolysis temperature generally shifted the 5dSCAN-Si concentration higher at 550 °C, particularly in biochars with greater alkali pretreatment. For example, in the KOH-enhanced rice straw biochar, the 10KB prepared at 550 °C yielded 5dSCAN-Si content of 4.67%, which was significantly higher than the 10KB prepared at 350 and 450 °C by 110 and 61%, respectively. The 5dSCAN-Si content of the 10K2B and 10CB treatments prepared at 550 °C was also 61 and 62% higher than that of those prepared at 350 °C (Fig. 2A). A similar trend was seen for the rice husk biochars (Fig. 2B). Interestingly, the extractable Si content of non-enhanced rice husk 0B by 5dSCAN method was less than that of rice straw 0B samples. In addition, the 5dSCAN-Si content of biochars pretreated with KOH and K_2CO_3 increased significantly with increasing pyrolysis temperature; however, the 5dSCAN-Si content of 5CB and 10CB biochars pretreated with CaO remained relatively stable.

Figure 3 shows the comparison of extractable Si level in alkali-enhanced biochar sources by four additional extraction methods. Since high alkali pretreatment yielded higher Si extractability, only 10KB, 10K2B, and 10CB were selected in this comparison along with feedstock, 0B and wollastonite (WO), which was used as a standard Si fertilizer. The 0.5 M HCl method extracted significantly more Si from wollastonite than that from biochars produced at all three pyrolysis temperatures, regardless of which biomass feedstocks were used. On the other hand, the 1hSCAN method extracted significantly more Si from alkali-enhanced biochars made from both feedstocks, especially rice straw, than that from wollastonite. The 1hSCAN method yielded equivalent or even more extractable Si from alkali-enhanced biochars made at 350 and 550 °C than that from the 0.5 M

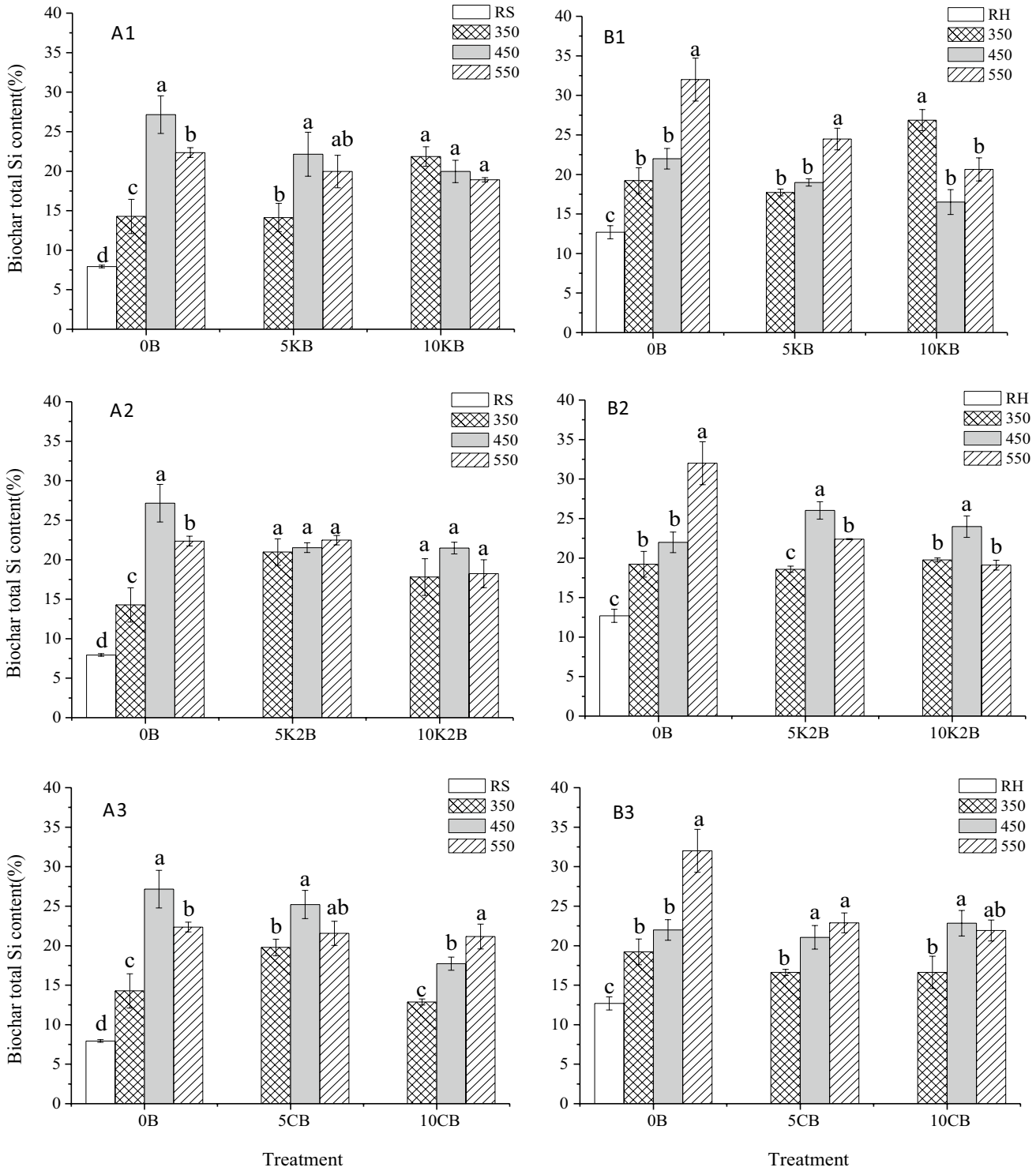

Fig. 1 Total Si contents of (**A**) rice straw biochar and (**B**) rice husk biochar prepared at different pyrolysis temperatures. Subgraphs A1 and B1, A2 and B2, A3 and B3 indicate alkali treatments with KOH, K_2CO_3, or CaO, respectively; RS, rice straw; RH, rice husk; 0B, 5KB/5K2B/5CB, 10KB/10K2B/10CB indicate the biochars prepared at the proportion of KOH/K_2CO_3/CaO to feedstock of 0:100, 5:100, 10:100. The 350, 450, 550 °C indicate pyrolysis temperatures. Different letters indicate significant differences within treatments ($P < 0.05$). The error bar indicates plus and minus of one standard deviation

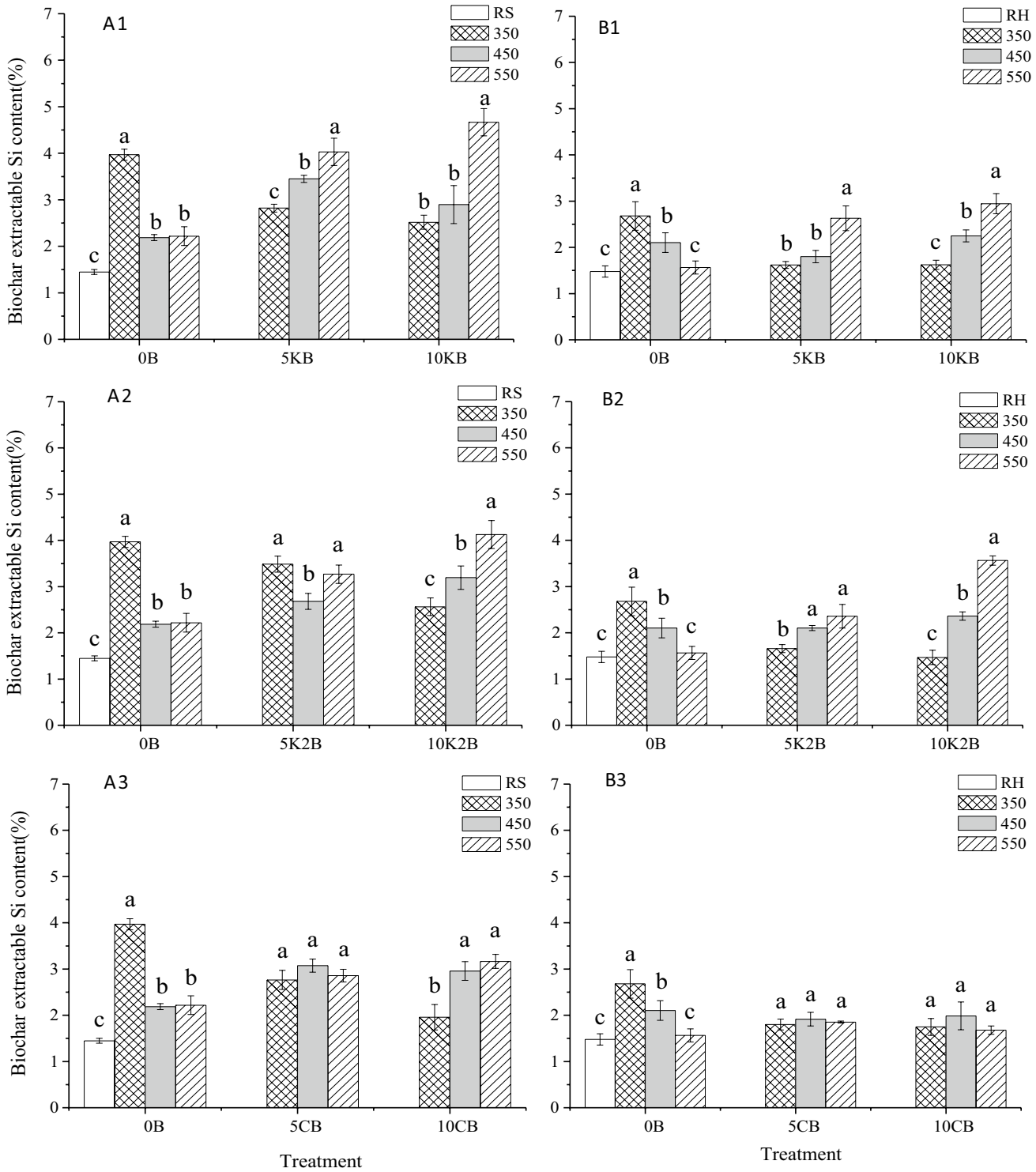

Fig. 2 Comparison of 5dSCAN-extractable Si contents of alkali-enhanced (**A**) rice straw and (**B**) rice husk biochars prepared at different pyrolysis temperatures. Subgraphs A1 and B1, A2 and B2, A3 and B3 indicate alkali treatments with KOH, K_2CO_3, or CaO, respectively; RS, rice straw; RH, rice husk; 0B, 5KB/5K2B/5CB, 10KB/10K2B/10CB indicate the biochars prepared at the proportion of KOH/K_2CO_3/CaO to feedstock of 0:100, 5:100, 10:100. The 350, 450, 550 °C indicate pyrolysis temperatures. Different letters indicate significant differences within treatment ($P < 0.05$). The error bar indicates plus and minus of one standard deviation

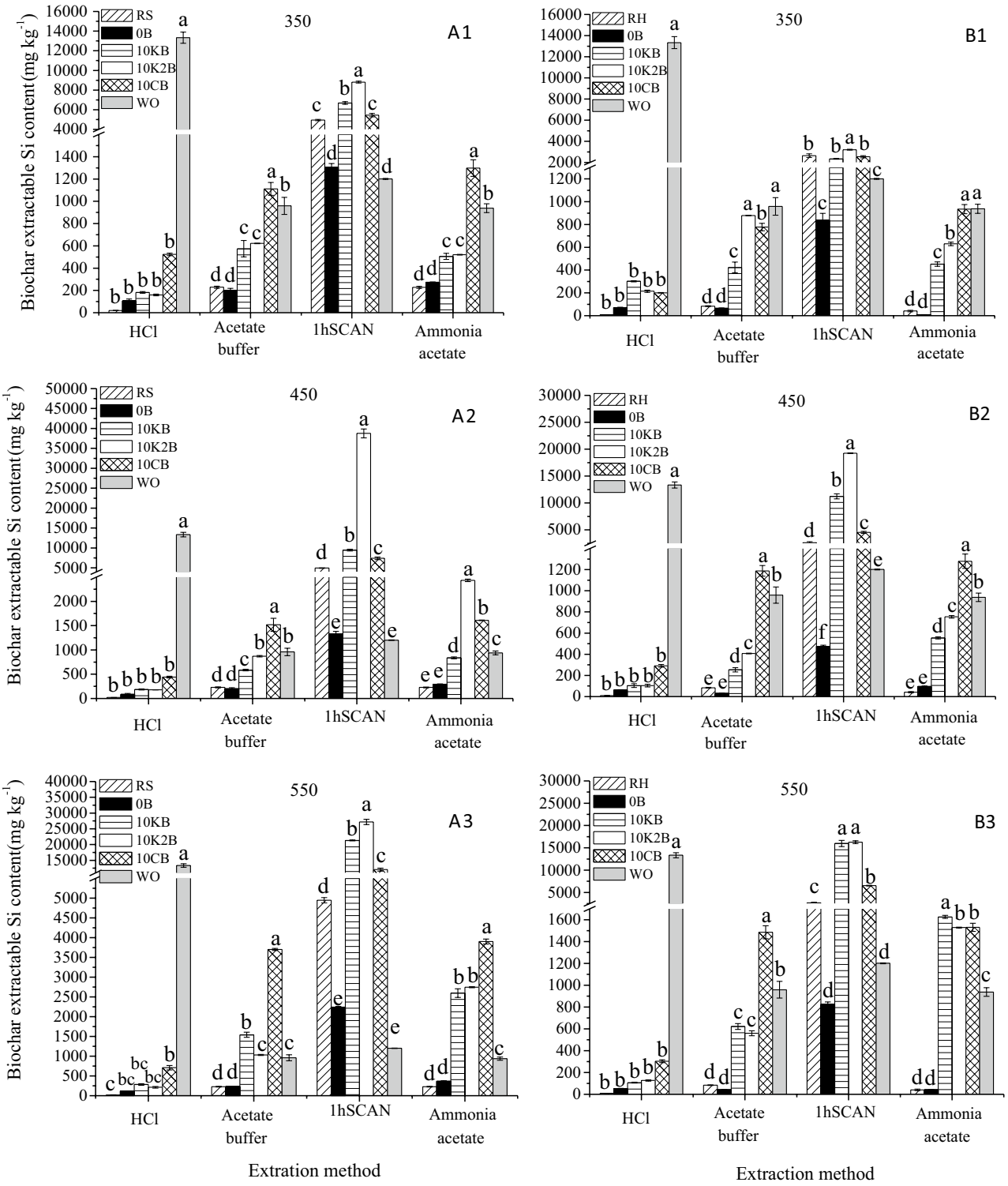

Fig. 3 Alkali-enhanced (**A**) rice straw and (**B**) husk biochar extractable Si extracted from four routine extraction methods. Subgraphs A1 and B1, A2 and B2, A3 and B3 indicate pyrolysis temperatures of 350, 450, 550 °C, respectively; RS, rice straw; RH, rice husk; 0B, 10KB/10K2B/10CB indicate the biochars prepared at the proportion of $KOH/K_2CO_3/CaO$ to feedstock of 0:100, 10:100.; *WO* wollastonite. Different letters indicate significant differences within treatment ($P < 0.05$). The error bar indicates plus and minus of one standard deviation

HCl extraction of wollastonite (Fig. 3). This was particularly evident for the 10K2B, 10KB, and 10CB treatments prepared at 550 °C, which showed the increase of 1hSCAN-Si content of 2163, 1675, and 903% higher than wollastonite, respectively. Furthermore, both 1 M sodium acetate buffer and 0.5 M ammonium acetate methods generally extracted less Si compared to the 1hSCAN extraction procedure but they extracted more Si from alkali-enhanced biochars than that from wollastonite as well as from non-enhanced 0B samples. These four additional test methods also showed that alkali-enhanced biochars tended to have greater extractable Si concentrations when produced at higher pyrolysis temperatures, and extractable Si concentrations were generally significantly higher than those of non-enhanced 0B biochars. Overall, these methods measure various fractions of extractable Si from different Si sources. Nonetheless, it was found that the Si fraction extracted by 0.5 M HCl was closely related to that extracted by the buffered sodium acetate (pH 4.0) ($r=0.967$, $P<0.01$), whereas the 1hSCAN extraction method was related to 0.5 M ammonium acetate method ($r=0.978$, $P<0.01$). The 1 h and 5 day Na_2CO_3-NH_4NO_3 methods were only weakly related ($r=0.626$, $P<0.05$).

3.4 Si release from alkali-enhanced biochar prepared at different pyrolysis temperatures

Total Si released over 30 days from biochar prepared at different temperatures in unbuffered weak acid (0.1 mM HCl, pH 4.0) and neutral salt (0.01 M KCl, initially adjusted to pH 7.0) solutions are shown in Figs. 4 and 5, respectively. Since both total Si and 5dSCAN-Si contents of biochars were similar between KOH and K_2CO_3 pretreatments and were generally greater than those of the CaO pretreatment, only K_2CO_3-enhanced rice straw biochars were selected for this evaluation. In this assessment, the alkali-enhanced biochar was compared with 0B (non-enhanced), feedstock (RS) as well as with wollastonite and silica slag. For both acid and neutral salt solutions, the 10K2B biochar showed the greatest cumulative Si release, followed by 5K2B biochar. The Si release from the both was higher than that from the 0B biochar as well as that from the raw feedstock, wollastonite and silica slag over the 30-day incubation. The 30-day cumulative Si release in the unbuffered weak acid and neutral salt solutions was highly correlated ($r=0.927$, $P<0.05$ for rice straw biochars and $r=0.995$, $P<0.01$ for husk biochars, respectively). A higher pyrolysis temperature generally led to greater Si release, with 450 and 550 °C-prepared biochars yielding greater Si release than 350 °C prepared biochar.

The Si release characteristics suggested that these samples could be divided into three groups: (1) the RS, WO and SL group that released the least Si over 30 days and for which Si release curves were close to each other or mostly overlapped, (2) the K_2CO_3-enhanced biochar (5K2B and 10K2B) group, which showed a rapid Si release during the first 2 days, continued to release gradually with time and had the greatest Si release among all treatments, and (3) the 0B biochars, which yielded Si release curves between those of the other two groups. It is interesting to note that the Si release curves and the cumulative release from the rice straw 0B biochars were closer to those of the K_2CO_3-enhanced biochars for rice straw feedstock (Figs. 4A and 5A), while the rice husk 0B samples were not to their K_2CO_3-enhanced biochars for rice husk (Figs. 4B and 5B), indicating a difference in the nature of Si release between the two biochar feedstocks in responding to alkali pretreatment.

3.5 Effect of alkali-enhanced biochar application on rice Si uptake and yield

Rice growth in soils treated with alkali-enhanced biochars along with non-enhanced biochar (0B) produced at different temperatures was evaluated in a greenhouse potting study, and the results are presented in Figs. 6 and 7. Based on the amount of Si extracted by different chemical methods and the cumulative Si release studies (Figs. 2, 3, 4 and 5), the potting trial focused only on a comparison of K_2CO_3-enhanced biochar with non-enhanced 0B biochar, wollastonite, and silica slag. Application of biochars significantly increased the Si content of rice straw compared to that of the control (CK) treatment. The Si uptake under the treatments of rice straw biochars, RS-10K2B-350 and RS-10K2B-550, was 31 and 29% higher than that of the control treatment, respectively (Fig. 6A). The Si uptake under the treatment of rice husk biochar RH-10K2B-550 was the highest among all Si treatments and was significantly higher than wollastonite and calcium silicate slag by 34 and 24%, respectively (Fig. 6B). In addition, for the rice husk-derived biochar treatments, the Si uptake contents in straw associated with the RH-0B-550 and RH-10K2B-550 treatments were significantly higher than those of the corresponding RH-0B-350 and RH-10K2B-350 treatments by 9 and 33%, respectively. These results indicated that alkali-enhanced biochar Si sources prepared at high pyrolysis temperatures tended to promote higher Si uptake by rice straw, particularly in the case of the rice husk-derived biochar products. Furthermore, the alkali-enhanced biochar Si sources also increased rice grain yields. Applications of both RS- and RH-10K2B-550 biochars produced significantly higher rice grain yields than those of non-enhanced RS- and RH-0B-350 biochars (Fig. 7). The RH-10K2B-550 application had significantly higher rice yield than the RH-0B-550 treatment, while RS-10K2B-550 had greater yield than RS-0B-550 (Fig. 7). In addition, RH-10K2B-350 treatment led to a rice yield that was numerically higher than the yield of the RH-0B-350 treatment. Rice yield associated with the RH-10K2B-550 treatment

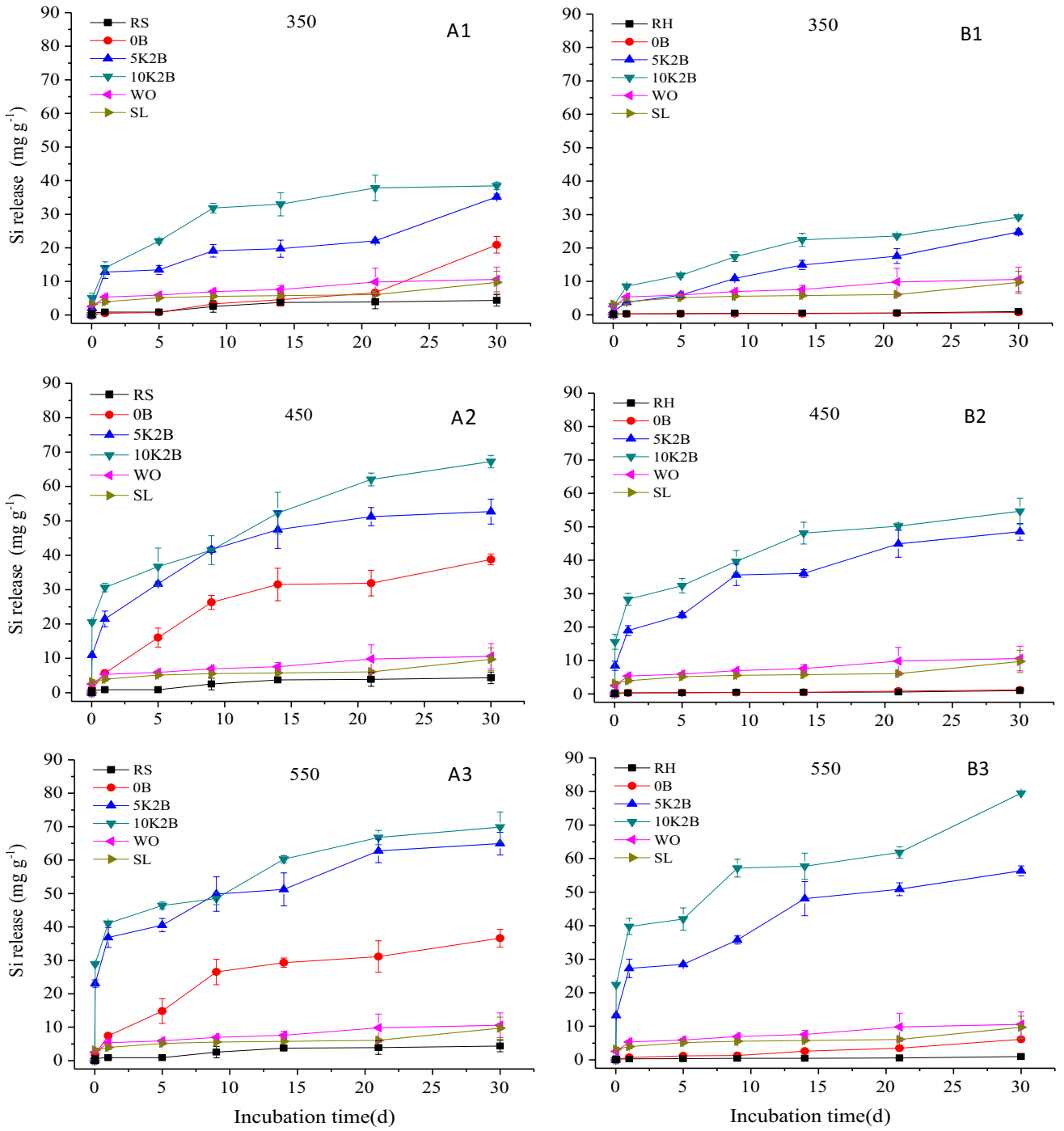

Fig. 4 Si release of K_2CO_3-enhanced (**A**) rice straw and (**B**) rice husk biochars over 30 days in unbuffered weak acid (0.1 mM HCl) solutions. Subgraphs A1 and B1, A2 and B2, A3 and B3 indicate pyrolysis temperatures of 350, 450, 550 °C, respectively. RS, rice straw; RH, rice husk; 0B, 5K2B and 10K2B indicate the biochars prepared at the proportion of K_2CO_3 to feedstock of 0:100, 5:100 and 10:100; *WO* wollastonite, *SL* calcium silicate slag. The error bar indicates plus and minus of one standard deviation

was even significantly greater than that of wollastonite and silica slag amendments. Grain yield was significantly correlated with Si uptake in rice straw ($r = 0.808$, $P < 0.01$) for biochar Si sources of RS/RH-0B-350/550 and RS/RH-10K2B-350/550 treatments (Fig. S2). These results indicate that both pyrolysis temperature and alkali-pretreatment are important in producing biochar-based Si fertilizer source. These results were consistent with greater cumulative dissolution of Si in both weak acid and unbuffered neutral salt solutions from the alkali-enhanced

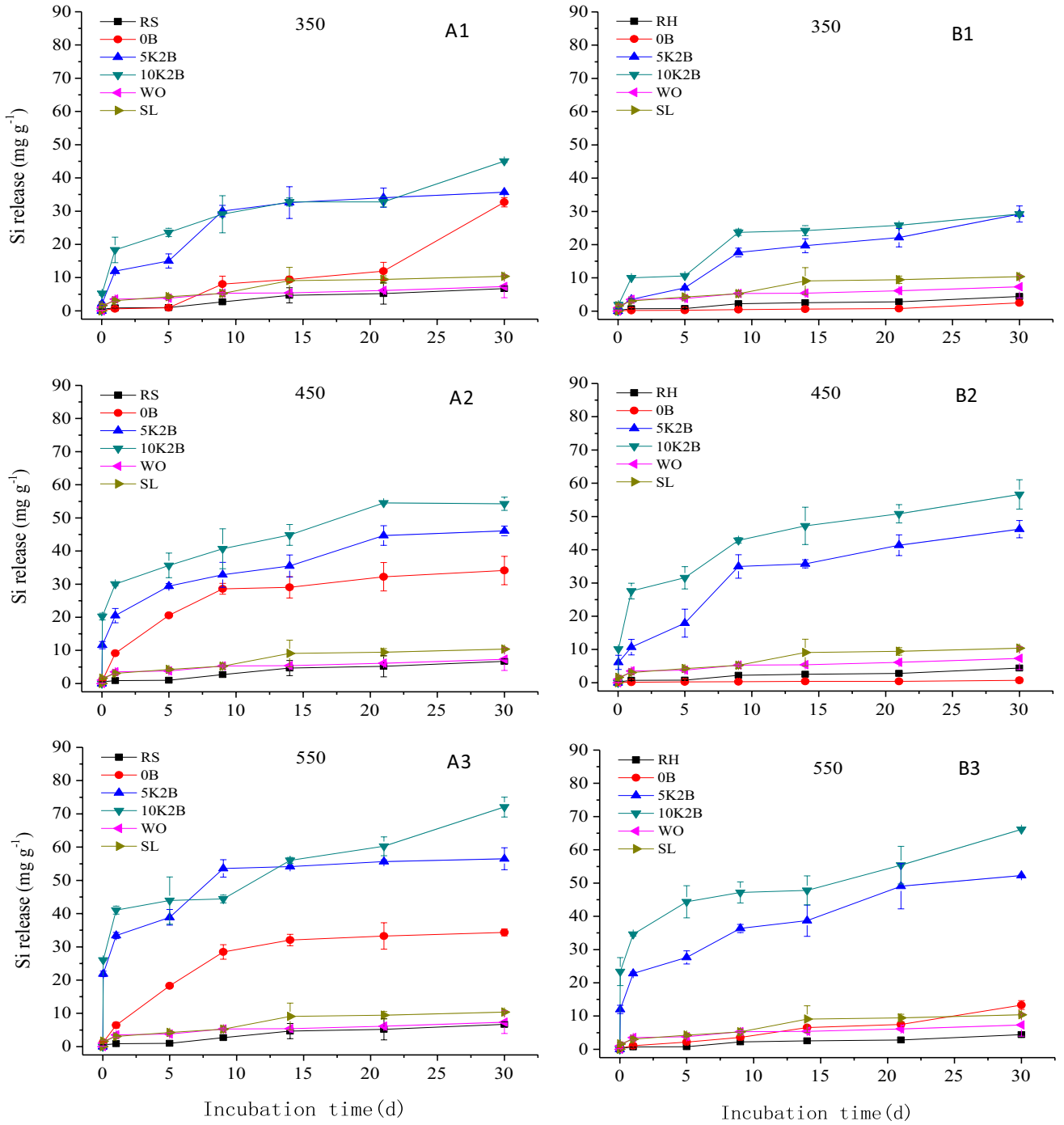

Fig. 5 Si release of K_2CO_3-enhanced (**A**) rice straw and (**B**) rice husk biochars over 30 days in unbuffered neutral salt (0.0 1 M KCl) solutions. Subgraphs A1 and B1, A2 and B2, A3 and B3 indicate pyrolysis temperatures of 350, 450, 550 °C, RS, rice straw; RH, rice husk; 0B, 5K2B and 10K2B indicate the biochars prepared at the proportion of K_2CO_3 to feedstock of 0:100, 5:100 and 10:100; *WO* wollastonite, *SL* calcium silicate slag. The error bar indicates plus and minus of one standard deviation

10K2B biochar produced at 550 °C (Figs. 4 and 5). Rice grain yield was closely related to cumulative Si release over 30 days ($Y = 0.0072X + 0.724$, $r = 0.924$, $P < 0.01$ for release in weak acid and $Y = 0.0091\ X + 0.671$, $r = 0.890$, $P < 0.01$ in unbuffered neutral solution) (Please see supplementary Figs. S3 and S4).

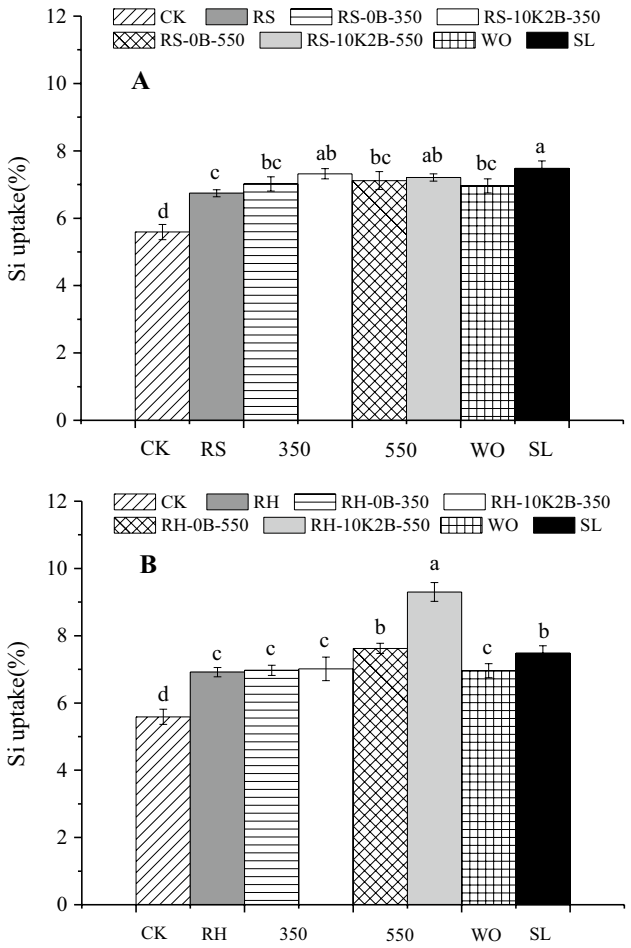

Fig. 6 Rice Si uptake with alkali-enhanced (**A**) rice straw biochar and (**B**) rice husk biochar amendments. CK, no amendment; RS/RH, rice straw/husk; RS/RH-0B-350 and RS/RH-10K2B-350 are rice straw and husk biochars prepared with the proportion of K_2CO_3 to feedstock at 0 and 10 at 350 °C, respectively; RS/RH-0B-550 and RS/RH-10K2B-550 are rice straw biochars prepared with the proportion of K_2CO_3 to feedstock at 0 and 10 at 550 °C, respectively; *WO* wollastonite, *SL* silicate calcium slag. The error bar indicates plus and minus of one standard deviation

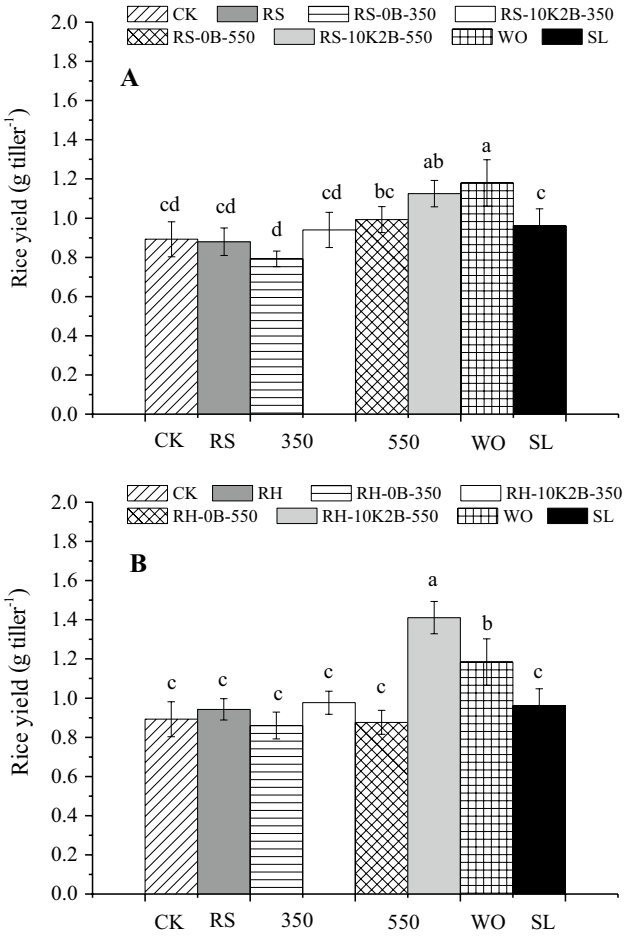

Fig. 7 Rice yield with alkali-enhanced (**A**) rice straw biochar and (**B**) rice husk biochar amendments. CK, non-amendment; RS/RH, rice straw/husk; RS/RH-0B-350 and RS/RH-10K2B-350 are rice straw and husk biochars prepared with the proportion of K_2CO_3 to feedstock at 0 and 10 at 350 °C, respectively; RS/RH-0B-550 and RS/RH-10K2B-550 are rice straw biochars prepared with the proportion of K_2CO_3 to feedstock at 0 and 10 at 550 °C, respectively; *WO* wollastonite, *SL* silicate calcium slag. The error bar indicates plus and minus of one standard deviation

4 Discussion

4.1 Effect of pyrolysis temperature and alkali treatment on biochar chemical and physical properties

As pyrolysis temperature increased from 350 to 550 °C, the yield of both non-enhanced (0B) and alkali-enhanced biochars from rice straw and husk sharply decreased (Tables S1 and S2), due to increasing decomposition of lignocellulosic materials in biomass (Paris et al. 2005). This result is similar to studies of wood, rice husk and sugarcane bagasse biochars produced at different pyrolysis temperatures (Kim et al. 2012; Keiluweit et al. 2010; Jeong et al. 2016; Suliman et al. 2016; Nwajiaku et al. 2018). In addition, alkali-enhanced biochars from both rice straw and rice husk increased the pH and ash content as pyrolysis temperature increased from 350 to 550 °C, consistent with non-enhanced biochar (0B). The latter was attributed to the conversion of alkali and alkaline earth cations (Ca, Mg, K, Na) to alkaline substances such as oxides, hydroxides, chlorides, and carbonates and the loss of acidic functional groups (Novak et al. 2009; Van Zwieten et al. 2010; Ahmad et al. 2012). Higher ash content was generally observed with alkali pretreatment of larger proportion of KOH, K_2CO_3 and CaO. On the other hand, the effect of pyrolysis temperature on the C content of alkali-enhanced biochar was less consistent, although C concentration in the non-enhanced biochar (0B) generally increased, which has been widely reported along with increase in concentrations

of inorganic elements (Novak et al. 2009; Laird 2008; Jeong et al. 2016). The increase in alkali pretreatment proportion generally decreased biochar C content. Between 350 and 450 °C pyrolysis temperature, alkali pretreatment showed inconsistent changes in biochar C content. However, at 550 °C, C content of KOH-enhanced biochars generally decreased compared to 0B biochar samples (Tables S1 and S2). This was likely due to a removal of more non-fixed carbon in feedstock biomass by KOH during pyrolysis (Huang et al. 2017) and a relative increase in the mass of alkali agent as ash components (Agrafioti et al. 2013). In addition, as expected, biochar total K and Ca contents were significantly elevated with specific amendment ratio of KOH, K_2CO_3 and CaO, respectively. Overall, similar to non-enhanced biochar, all three alkali pretreatments affected the output yield, ash content, and pH as well as part of elemental composition of prepared biochars at different pyrolysis temperatures. Also, the significantly enhanced total K content of KOH and K_2CO_3-enhanced biochars could function as K source in soil biochar amendment.

Several studies have investigated the influence of alkali agents on biomass C transformation during pyrolysis (Azargohar and Dalai 2006; Chen et al. 2020; Yang et al. 2020; Zhao et al. 2020). In general, decarboxylation reaction was known as the main process to remove C from feedstock during pyrolysis and it had similar preference for biomass as dehydration reaction under low temperature pyrolysis (Liu and Han 2015). In addition, decarboxylation reaction was shown to dominate at pyrolysis temperature above 350 °C, whereas decarbonylation reaction was at above 450 °C (Zhang et al. 2020). At 550 °C, biochar exhibited stable characteristic atomic ratios of H/C < 0.4 and O/C < 0. 2 (Jeong et al. 2016) and significant fusion into aromatic ring structure (Zhang et al. 2020). The higher pyrolysis temperature mainly promoted the decomposition of the volatiles into the gaseous products while did not promote the decomposition of biochar significantly (Zhang et al. 2020). In our study, the clear decrease in C contents of alkali-enhanced biochars at 550 °C compared to 0B biochars indicated the significant role of alkali pretreatment (Tables S1 and S2). Alkali agent such as KOH was found to promote dehydration, decarboxylation, and decarbonylation reactions with biomass during pyrolysis (Yang et al. 2020; Zhao et al. 2020). The KOH treatment could enhance the decomposition of volatile intermediate, strengthen the reaction with stable C fragments, and facilitate the overall reaction rate with C matrix of biomass (Azargohar and Dalai 2006; Chen et al. 2020).

4.2 Effect of pyrolysis temperature and alkali treatment on biochar phytolith-Si release

Biochar total Si content generally increased with increasing pyrolysis temperature. However, total Si content of some treatments such as RS-5KB and RH-5K2B decreased from 450 to 550 °C. The loss was probably due to the formation of trace silica scale sticking to the wall of crucible during the production of alkali-enhanced biochar. Similar trend of lower total Si content was also observed when biochar pyrolysis temperature increased from 300 to 700 °C (Huang et al. 2020).

Non-enhanced biochar (0B) samples showed the higher 5dSCAN-Si content at 350 °C pyrolysis temperature, and it had lower extractable Si as pyrolysis temperature was increased to 550 °C (Fig. 2). This result was consistent with the research of Xiao et al. (2014), who reported higher Si dissolution release from pristine rice straw biochar of 350 °C than that of biochars prepared at lower (150–250 °C) and higher (500–700 °C) pyrolysis temperatures. Nguyen et al. (2014) also reported higher Si dissolution from rice straw ashing at 400 °C than that at 600–800 °C. Based on various spectroscopic analyses of structure, morphology and species, Xiao et al. (2014) proposed a C–Si–C structure model to explain this phenomenon. According to these authors, polymerization of monosilicic acid dominated at < 250 °C through dehydration to result in a dense C–Si–C structure in biochar. As pyrolysis temperature was increased to 350 °C, the outermost C layer began to crack, exposing the inner Si layer of C–Si–C structural configuration and generating a large amount of dissolved Si. At 500–700 °C, the C layer of C–Si–C structure was further detached. However, due to crystallization of Si, the cumulative release of dissolved Si was less than biochar produced at 350 °C (Xiao et al. 2014; Wang et al. 2018b). The C–Si coupling interaction in response to pyrolysis temperature change was further suggested as the mechanism for mutual protection between Si and C from dissolution and responsible for biochar C stability (Guo and Chen 2014; Wang et al. 2019b). The enhanced BC stability at pyrolysis temperature at above 500 °C was attributable to the increased aromaticity along with Si encapsulation of C and Si components changing from amorphous to crystalline and from metastable α-quartz to stable β-quartz phase, which is intertwined with C (Guo and Chen 2014). In our study, through alkali pretreatment, 5dSCAN-Si content of resulting biochars was clearly increased as evidenced in 10KB, 10K2B and 10CB samples as pyrolysis temperature was increased from 350 to 550 °C (Fig. 2). In a previous study, we explored the release mechanism of phytolith-Si in alkali-enhanced biochar at 550 °C and showed that alkali such as KOH pretreatment could significantly damage the dumbbell structures of phytoliths that are stacked in layers by exposing the outermost layers of phytoliths for Si release (Wang et al. 2018a). Liu et al. (2012) also indicated that KOH could be embedded into the interior of phytolith and react with SiO_2 to generate less stable silicate as:

$$2KOH + SiO_2 \rightarrow K_2SiO_3 + H_2O \quad (1)$$

It is well known that K_2SiO_3 dissolution is much greater than SiO_2 due to the change in silicate structure from three-dimensional tectosilicate to single-chained inosilicate (Sparks 2003). While increased pyrolysis temperature could accelerate the burst of C layer of C–Si–C structural configuration and expose Si in the inner layer (Xiao et al. 2014), the enhanced contact of alkali reagents with inner Si layer accelerated the Si dissolution rather than Si crystallization in biochar (Fig. S1). The SEM–EDX image and elemental mapping clearly showed bleaching out of photolith-Si with KOH treatment while CaO treatment had less impact due to weak base nature and that CaO tended to stay on phyolith structural surface (Fig. S1). The latter likely explained the trend reversal in 5dSCAN-extractable Si of 10KB, 10K2B and 10CB as compared to 0B samples over increasing pyrolysis temperature.

The higher 5dSCAN-extractable Si content in alkali-enhanced biochars compared to non-enhanced biochars as influenced by pyrolysis temperature was also supported by cumulative release of Si over 30 days in unbuffered weak acid and neutral salt solutions (Figs. 4 and 5). Among rice husk and straw biochars prepared at different pyrolysis temperatures, alkali-enhanced biochars (5K2B and 10K2B) had the highest Si release in unbuffered weak acid and neutral salt solutions, and was also higher than feedstocks (RS and RH) and conventional Si fertilizers (WO and SL). The increase in pyrolysis temperature generally significantly increased Si release of alkali-enhanced 5K2B and 10K2B samples while it had less effect on non-enhanced 0B samples. This was consistent with the result of 5dSCAN-extractable Si content of alkali-enhanced biochars prepared at different temperatures (Fig. 2). These results further indicate the importance of alkali pretreatment, especially K_2CO_3, and appropriate higher pyrolysis temperature (550 °C) in preparing biochar Si fertilizer.

4.3 Effect of pyrolysis temperature on Si uptake from alkali-enhanced biochar

The unique Si dissolution and release characteristics of biochar with higher Si dissolution at 350–400 °C than the temperature out of this range noted by Xiao et al. (2014) and Nguyen et al. (2014) suggested that pyrolysis temperature could be an important factor to control Si release of biochars in soil. This phenomenon was, however, never examined previously through plant response, although several studies demonstrated that biochar made from Si-rich waste biomass could be used as a Si fertilizer source (Houben et al. 2014; Liu et al. 2014; Li et al. 2014, 2018; Abbas et al. 2017). Most biochars used as soil amendment for agronomic application were prepared at temperatures greater than 450 °C to enhance C stability and to improve soil water and nutrient retention (Laird 2008; Spokas et al. 2012; Jeong et al. 2016). On the other hand, Wang et al. (2018a) showed that alkali-enhanced biochar could significantly increase extractable Si content of phytolith-rich biochars using AAPFCO-designated 5dSCAN extraction method for Si fertilizer evaluation. In this study, the greenhouse potting trial clearly showed that amendments of all biochars increased rice straw Si content. Treatment of the soil with alkali-enhanced rice husk biochar prepared at 550 °C (RH-10K2B-550) led to the highest Si uptake, greater than that of wollastonite and slag (Fig. 6). Most importantly, the same biochar treatment also showed the highest grain yield increase among all biochar amendments and had comparable or higher grain yield than the wollastonite and slag treatments (Fig. 7). The higher grain yield was correlated with the greater cumulative Si release in unbuffered weak acid and neutral salt solutions from alkali-enhanced biochars at 550 °C than from those prepared at 350 °C or from non-enhanced biochars (0B) (Figs. 4 and 5).

In addition, the difficulty in indexing fertilizer Si sources should be pointed out. Although different chemical methods have been used to evaluate fertilizer Si sources, various studies showed no single extraction that could predict Si availability (Haynes et al. 2013; Zellner et al. 2015). Therefore, the specific response of plant growth is especially important for evaluating different Si sources, particularly when it comes to biochar-based Si fertilizer. A recent study indicated that the chemical methods that could extract more Si quantitatively from both mineral fertilizers and biomass-based thermal products as well as could reproduce soil root conditions by buffering pH close to neutral likely do better in correlating with plant Si uptake (Duboc et al. 2019). In our study, we used unbuffered weak acid (0.1 mM HCl) and neutral salt solution (0.01 M KCl) to assess Si release over 30 days. The 30-day cumulative Si release in the unbuffered 0.1 mM HCl and 0.01 M KCl solutions showed good correlations with rice straw Si uptake ($r = 0.879$ and 0.881, $P < 0.05$, respectively). In addition, they were strongly correlated with rice grain yields ($r = 0.924$ and 0.890, $P < 0.01$, respectively) (Figs. S3 and S4). Among the four extraction methods, 1hSCAN and ammonium acetate extractions were found most closely correlated with rice yield ($r = 0.708$, $P < 0.05$). Nonetheless it was clear that alkali-enhanced biochar at 550 °C, especially K_2CO_3 pretreatment, facilitated better rice Si uptake and grain yield than the non-enhanced biochars or biochars prepared at lower temperatures.

It should be pointed out while the enhanced phytolith-Si solubility of biochar by alkali pretreatment likely primarily contributed to the greater rice Si uptake and higher yield, the potentially stronger interaction between biochar and rice roots could play a role. Recent work suggested that biochar amendment could cause an increase in electrical potential difference between rice root membrane and soil due to

increased soil E_h and pH, which improves nutrient uptake (Quin et al. 2015; Sun et al. 2017; Chew et al. 2020). Biochar particles were found to be embedded into the plaque layer formed on rice roots and root hairs could enter the pores of biochar (Joseph et al. 2013). According to Zeng et al. (2014) and Haruta et al. (2018), O_2, K^+ and pH are some of key environmental factors influencing plant root membrane potentials. Although we did not measure rhizosphere E_h change in potting study, the generally high pH and K content of alkali-enhanced biochars used in the study (Table S1) would be expected to increase root membrane/soil potential difference due to increased soil E_h with increasing pH, which drives nutrient uptake (Chew et al. 2020; Zeng et al. 2014). Sufficient K nutrient could ensure K^+-signaling that mediates plant-adaptive response to environment including those of Si-specific transporters (Hosseini et al. 2017). Both could help improve Si uptake as monosilicic acid uptake besides solubilizing phytoliths-Si.

5 Conclusion

This study demonstrated the influence of pyrolysis temperature on the Si release of alkali-enhanced biochars. Different from unenhanced biochar, which generally showed higher chemically extractable Si when prepared at 350 °C, alkali-enhanced biochar, especially with KOH or K_2CO_3, tended to have higher extractable Si when it was prepared at 550 °C. In addition, biochar prepared with K_2CO_3 pretreatment at 550 °C released more Si to weak acid and unbuffered neutral salt solutions over 30 days. The greenhouse potting trial also showed that rice plants responded, with greater Si uptake and grain yield, to alkali-enhanced biochar. Overall, 550 °C was the better pyrolysis temperature to prepare alkali-enhanced biochar that could increase Si release for plant growth as compared to 350 or 450 °C. Additionally, KOH- or K_2CO_3-enahnced biochar can provide K source besides enhanced C stability.

Supplementary Information The online version contains supplementary material available at https://doi.org/10.1007/s42773-021-00112-3.

Acknowledgements This work was, in part, supported by the Louisiana Board of Regents Support Fund #LEQSF(2017–18)-RD-D02 and #LEQSF(2019–20)-RD-D-01, the USDA National Institute of Food and Agriculture Hatch Project #1013888, and the Shaanxi University of Technology Talent Startup Program (SLGRC19), Hanzhong, Shaanxi, China.

Declarations

Conflict of interests The authors have no conflicts of interest to declare that are relevant to the content of this article.

References

Abbas T, Rizwan M, Ali S, Zia-ur-Rehman M, Qayyum MF, Abbas F, Hannan F, Rinklebe J, Ok YS (2017) Effect of biochar on cadmium bioavailability and uptake in wheat (Triticum aestivum L.) grown in a soil with aged contamination. Ecotoxicol Environ Saf 140:37–47. https://doi.org/10.1016/j.ecoenv.2017.02.028

Adrees M, Ali S, Rizwan M, Zia-ur-Rehman M, Ibrahim M, Abbas F, Farid M, Qayyum MF (2015) Mechanisms of silicon-mediated alleviation of heavy metal toxicity in plant: a review. Ecotoxicol Environ Saf 119:186–197. https://doi.org/10.1016/j.ecoenv.2015.05.011

Agrafioti E, Bouras G, Kalderis D, Diamadopoulos E (2013) Biochar production by sewage sludge pyrolysis. J Anal Appl Pyrol 101:72–78. https://doi.org/10.1016/j.jaap.2013.02.010

Ahmad M, Lee SS, Dou X, Mohan D, Sung JK, Yang JE, Ok YS (2012) Effects of pyrolysis temperature on soybean stover- and peanut shell-derived biochar properties and TCE adsorption in water. Bioresour Technol 118(8):536–544. https://doi.org/10.1016/j.biortech.2012.05.042

Azargohar R, Dalai AK (2006) Biochar as a precursor of activated carbon. Humana Press Inc, pp 762–773. https://doi.org/10.1007/978-1-59745-268-7-62

Bao SD (2000) Soil agro-chemistry analysis, 3rd edn. China Agriculture Press, Beijing (**in Chinese**)

Cantrell KB, Hunt PG, Uchimiya M, Novak JM, Ro KS (2011) Impact of pyrolysis temperature and manure source on physicochemical characteristics of biochar. Bioresour Technol 107:419–428. https://doi.org/10.1016/j.biortech.2011.11.084

Chen W, Gong M, Li K, Xia M, Chen Z, Xiao H, Fang Y, Chen Y, Yang H, Chen H (2020) Insight into KOH activation mechanism during biomass pyrolysis: Chemical reactions between O-containing groups and KOH. Appl Energy 278:115730. https://doi.org/10.1016/j.apenergy.2020.115730

Chew J, Zhu L, Nielsen S, Graber E, Mitchell DRG, Horvat J, Mohammed M, Liu M, Zwieten L, Fan X (2020) Biochar-based fertilizer: supercharging root membrane potential and biomass yield of rice. Sci Total Environ 713:136431. https://doi.org/10.1016/j.scitotenv.2019.136431

Duboc O, Robbe A, Santner J, Folegnani G, Gallais P, Lecanuet C, Zehetner F, Nagl P, Wenzel WW (2019) Silicon availability from chemically diverse fertilizers and secondary raw materials. Environ Sci Technol 53(9):5359–5368

Epstein E (2009) Silicon: its manifold roles in plants. Ann Appl Biol 155:155–160. https://doi.org/10.1111/j.1744-7348.2009.00343.x

Fraysse F, Pokrovsky OS, Schott J, Meunier JD (2006) Surface properties, solubility and dissolution kinetics of bamboo phytoliths.

Geochim Cosmochim Acta 70:1939–1951. https://doi.org/10.1016/j.gca.2005.12.025
Guntzer F, Keller C, Meunier JD (2012) Benefits of plant silicon for crops: a review. Agron Sustain Dev 32:201–213. https://doi.org/10.1007/s13593-011-0039-8
Guo J, Chen B (2014) Insights on the molecular mechanism for the recalcitrance of biochars: interactive effects of carbon and silicon components. Environ Sci Technol 48(16):9103–9112. https://doi.org/10.1021/es405647e
Hallmark C, Wilding L, Smeck N (1982) Methods of soil analysis. Part 2. Chemical and microbiological properties. American Society of Agronomy Inc, Madison, pp 263–273
Haruta M, Tan LX, Bushey DB, Swanson SJ, Sussman MR (2018) Environmental and genetic factors regulating localization of the plant plasmamembrane H+-ATPase. Plant Physiol 176:364–377. https://doi.org/10.1104/pp.17.01126
Haynes RJ, Belyaeva O, Kingston G (2013) Evaluation of industrial wastes as sources of fertilizer silicon using chemical extractions and plant uptake. J Plant Nutr Soil Sci 176:238–248. https://doi.org/10.1002/jpln.201200372
Hosseini SA, Maillard A, Hajirezaei MR, Ali N, Schwarzenberg A, Jamois F, Yvin J-C (2017) Induction of barley silicon transporter HvLsi1 and HvLsi2, increased silicon concentration in the shoot and regulated Starch and ABA homeostasis under osmotic stress and concomitant potassium deficiency. Front Plant Sci 8:1359. https://doi.org/10.3389/fpls.2017.01359
Houben D, Sonnet P, Cornelis JT (2014) Biochar from Miscanthus: a potential silicon fertilizer. Plant Soil 374:871–882. https://doi.org/10.1007/s11104-013-1885-8
Huang CYL, Schulte E (1985) Digestion of plant tissue for analysis by ICP emission spectroscopy. Soil Sci Plant Anal 16:943–958. https://doi.org/10.1080/00103628509367657
Huang H, Tang J, Gao K, He R, Zhao H, Werner D (2017) Characterization of KOH modified biochars from different pyrolysis temperatures and enhacned adsorptionn of antibiotics. RCS Adv 7:14640–14648. https://doi.org/10.1039/C6RA27881G
Huang F, Gao L, Wu R, Wang H, Xiao R (2020) Qualitative and quantitative characterization of adsorption mechanisms for Cd2+ by silicon-rich biochar. Sci Total Environ 731:139163. https://doi.org/10.1016/j.scitotenv.2020.139163
Iler KR (1979) The chemistry of silica. John Wiley & Sons, New York
Islam W, Tayyab M, Khalil F, Hua Z, Huang Z, Chen HYH (2020) Silicon-mediated plant defense against pathogens and insect pests. Pestic Biochem Physiol 168:104641. https://doi.org/10.1016/j.pestbp.2020.104641
Jeong CY, Dodla SK, Wang JJ (2016) Fundamental and molecular composition characteristics of biochars produced from sugarcane and rice crop residues and by-products. Chemosphere 142:4–13. https://doi.org/10.1016/j.chemosphere.2015.05.084
Joseph S, Graber ER, Chia C, Munroe P, Donne S, Thomas T, Nielse S, Marjo C, Rutlidge H, Pan GX, Li L, Taylor P, Rawal A, Hook J (2013) Shifting paradigms: development of high-efficiency biochar fertilizers based on nano-structures and soluble components. Carbon Management 4:323–343. https://doi.org/10.4155/cmt.13.23
Kato N, Owa N (1997) Dissolution of slag fertilizers in a paddy soil and Si uptake by rice plants. Soil Sci Plant Nutr 43:329–341. https://doi.org/10.1080/00380768.1997.10414757
Keiluweit M, Nico PS, Johnson MG (2010) Dynamic molecular structure of plant biomass-derived black carbon (biochar). Environ Sci Technol 44:1247–1253. https://doi.org/10.1021/es9031419
Kim J, Cho T, Choi JW (2012) Influence of pyrolysis temperature on physicochemical properties of biochar obtained from the fast pyrolysis of pitch pine (Pinus rigida). Bioresour Technol 118:158–162. https://doi.org/10.1016/j.biortech.2012.04.094
Korndörfer GH, Snyder GH, Ulloa M, Powell G, Datnoff LE (2001) Calibration of soil and plant silicon analysis for rice production. J Plant Nutr 24:1071–1084. https://doi.org/10.1081/PLN-100103804
Korndörfer GH, Pereira HS, Nolla A (2004) Analysis of silicon: soil, plant and fertilizer. Uberlandia, Brazil GPSi-ICIAG-UFU
Kuzyakov Y, Subbotina I, Chen H, Bogomolova I, Xu X (2009) Black carbon decomposition and incorporation into soil microbial biomass estimated by 14 C labeling. Soil Biol Biochem 41:210–219. https://doi.org/10.1016/j.soilbio.2008.10.016
Laird DA (2008) The charcoal vision: a win–win–win scenario for simultaneously producing bioenergy, permanently sequestering carbon, while improving soil and water quality. Agron J 100:178–181. https://doi.org/10.2134/agronj2007.0161
Li Z, Song Z, Cornelis JT (2014) Impact of rice cultivar and organ on elemental composition of phytoliths and the release of bioavailable silicon. Front Plant Sci 5:529. https://doi.org/10.3389/fpls.2014.00529
Li Z, Delvaux B, Yans J, Dufour N, Houben D, Cornelis J (2018) Phytolith-rich biochar increases cotton biomass and silicon-mineralomass in a highly weathered soil. J Plant Nutr Soil Sci 181:537–546. https://doi.org/10.1002/jpln.201800031
Liang YC, Ma TS, Li FJ, Feng YJ (1994) Silicon availability and response of rice and wheat to silicon in calcareous soils. Commun Soil Sci Plant Anal 25:2285–2297. https://doi.org/10.1080/00103629409369189
Linam F, McCoach K, Limmer MA, Seyfferth AL (2021) Contrasting effects of rice husk pyrolysis temperature on silicon dissolution and retention of cadmium (Cd) and dimethylarsinic acid (DMA). Sci Total Environ 765:144428. https://doi.org/10.1016/j.scitotenv.2020.144428
Liu Z, Han G (2015) Production of solid fuel biochar from waste biomass by low temperature pyrolysis. Fuel 158:159–165. https://doi.org/10.1016/j.fuel.2015.05.032
Liu P, Liu WJ, Jiang H, Chen JJ, Li WW, Yu HQ (2012) Modification of bio-char derived from fast pyrolysis of biomass and its application in removal of tetracycline from aqueous solution. Bioresour Technol 121:235–240. https://doi.org/10.1016/j.biortech.2012.06.085
Liu X, Li L, Bian R, Chen D, Qu J, Wanjiru KG, Pan G, Zhang X, Zheng J, Zheng J (2014) Effect of biochar amendment on soil-silicon availability and rice uptake. J Plant Nutr Soil Sci 177:91–96. https://doi.org/10.1002/jpln.201200582
Ma JF, Takahashi E (2002) Soil, fertilizer and plant silicon research in Japan. Elsevier Science, Dordrecht, The Netherlands
Meyer JH, Keeping MG (2001) Past, present and future research of the role of silicon for sugarcane in southern Africa. In: Datnoff LE, Snyder GH, Korndörfer GH (eds) Silicon in agriculture. Elsevier, Amsterdam, pp 257–275
Neumann D, Zur NU (2001) Silicon and heavy metal tolerance of higher plants. Phytochemistry 56:685–692. https://doi.org/10.1016/S0031-9422(00)00472-6
Nguyen BT, Lehmann J, Hockaday WC, Joseph S, Masiello CA (2010) Temperature sensitivity of black carbon decomposition and oxidation. Environ Sci Technol 44(9):3324–3331. https://doi.org/10.1021/es903016y
Nguyen N, Dulitz S, Guggenerger G (2014) Effects of pretreatment and solution chemistry on solubility of rice straw phytoliths. J Plant Nutr Soil Sci 177(3):349–359. https://doi.org/10.1002/jpln.201300056
NIAES (1987) Official methods of analysis of fertilizers, vol. 124. Tsukuba: National Institute of Agroenvironmental Sciences, Foundation Nohrin Kohsaikai, pp 36–37
Novak JM, Busscher WJ, Laird DL, Ahmedna M, Watts DW, Niandou MA (2009) Impact of biochar amendment on fertility of a

southeastern coastal plain soil. Soil Sci 174:105–112. https://doi.org/10.1097/SS.0b013e3181981d9a

Nwajiaku IM, Olanrewaju JS, Sato K, Tokunari T, Kitano S, Masunaga T (2018) Change in nutrient composition of biochar from rice husk and sugarcane bagasse at varying pyrolytic temperatures. Int J Recycl Org Waste Agricult 7(4):269–276. https://doi.org/10.1007/s40093-018-0213-y

Paris O, Zollfrank C, Zickler GA (2005) Decomposition and carbonisation of wood biopolymersda microstructural study of softwood pyrolysis. Carbon NY 43:53–66. https://doi.org/10.1016/j.carbon.2004.08.034

Quin P, Joseph S, Husson O, Donne S, Mitchell D, Munroe P, Phelan D, Cowie A, Van Zwieten L (2015) Lowering N2O emissions from soils using eucalypt biochar: the importance of redox reactions. Sci Rep 5:16773. https://doi.org/10.1038/srep16773

Saito K, Yamamoto A, Sa T, Saigusa M (2005) Rapid, micro-methods to estimate plant silicon content by dilute hydrofluoric acid extraction and spectrometric molybdenum method. Soil Sci Plant Nutr 51:29–36. https://doi.org/10.1111/j.1747-0765.2005.tb00003.x

Sebastian D, Rodrigues H, Kinsey C, Korndörfer G, Pereira H, Buck G, Datnoff LE, Miranda S, Provance-Bowley M (2013) A 5-day method for determination of soluble silicon concentrations in non-liquid fertilizer materials using a sodium carbonate-ammonium nitrate extractant followed by visible spectroscopy with heteropoly blue analysis: single-laboratory validation. J AOAC Int 96:251–259. https://doi.org/10.5740/jaoacint.12-243

Singh BP, Cowie AL, Smernik RJ (2012) Biochar carbon stability in a clayey soil as a function of feedstock and pyrolysis temperature. Environ Sci Technol 46(21):11770–11778. https://doi.org/10.1021/es302545b

Snyder GH (2001) Methods for silicon analysis in plants, soils, and fertilizers. In: Datnoff LE, Snyder GH, Korndörfer GH (eds) Silicon in agriculture. Elsevier, Amsterdam, pp 185–196

Sparks DL (2003) Environmental soil chemsitry, 2nd edn. Academic Press, New York

Spokas KA, Novak JM, Venterea RT (2012) Biochar's role as an alternative N-fertilizer: ammonia capture. Plant Soil 350:35–42. https://doi.org/10.1007/s11104-011-0930-8

Suliman W, Harsh JB, Abu-Lail NI, Fortuna A, Dallmeyer I, Garcia-Perez M (2016) Influence of feedstock source and pyrolysis temperature on biochar bulk and surface properties. Biomass Bioenergy 84:37–48. https://doi.org/10.1016/j.biombioe.2015.11.010

Sun TR, Levin BDA, Guzman JJL, Enders A, Muller DA, Angenent LT, Lehmann J (2017) Rapid electron transfer by the carbon matrix in natural pyrogenic carbon. Nat Commun 8:14873. https://doi.org/10.1038/ncomms14873

Takahashi K (1981) Effects of slags on the growth and the silicon uptake by rice plants and the available silicates in paddy soils. Bull Shikoku Agric Exp Stn 38:75–114

Van Zwieten L, Kimber S, Morris S, Chan K, Downie A, Rust J, Joseph S, Cowie A (2010) Effects of biochar from slow pyrolysis of papermill waste on agronomic performance and soil fertility. Plant Soil 327:235–246. https://doi.org/10.1007/s11104-009-0050-x

Wang JJ, Dodla SK, Henderson RE (2004) Soil silicon extractability with seven selected extractants in relation to colorimetric and ICP determination. Soil Sci 169:861–870. https://doi.org/10.1097/01.ss.0000149362.88935.8d

Wang M, Wang JJ, Wang X (2018a) Effect of KOH-enhanced biochar on increasing soil plant-available silicon. Geoderma 321:22–31. https://doi.org/10.1016/j.geoderma.2018.02.001

Wang Y, Xiao X, Chen B (2018b) Biochar impacts on soil silicon dissolution kinetics and their interaction mechanisms. Sci Rep 8:8040. https://doi.org/10.1038/s41598-018-26396-3

Wang M, Wang JJ, Tafti ND, Hollier CA, Myers G, Wang X (2019a) Effect of alkali-enhanced biochar on silicon uptake and suppression of gray leaf spot development in perennial ryegrass. Crop Prot 119:9–16. https://doi.org/10.1016/j.cropro.2019.01.013

Wang Y, Xiao X, Xu Y, Chen B (2019b) Environmental effects of silicon within biochar (sichar) and carbon-silicon coupling mechanisms: a critical review. Environ Sci Technol 53:13570–13582. https://doi.org/10.1021/acs.est.9b03607

Xiao X, Chen B, Zhu L (2014) Transformation, morphology, and dissolution of silicon and carbon in rice straw-derived biochars under different pyrolytic temperatures. Environ Sci Technol 48:3411–3419. https://doi.org/10.1021/es405676h

Yang H, Chen Z, Chen W, Chen Y, Wang X, Chen H (2020) Role of porous structure and active O-containing groups of activated biochar catalyst during biomass catalytic pyrolysis. Energy 210:118646. https://doi.org/10.1016/j.energy.2020.118646

Zellner W, Friedrich R, Kim S, Sturtz D, Frantz J, Altland J, Krause C (2015) Continuing assessment of the 5-day sodium carbonate ammonium nitrate extraction assay as an indicator test for silicon fertilizers. J AOAC Int 98(4):890–895. https://doi.org/10.5740/jaocint.14-205

Zeng F, Konnerup D, Shabala L, Zhou M, Colmer TD, Zhang G, Shabala S (2014) Linking oxygen availability with membrane potential maintenance and K+ retention of barley roots: implications for waterlogging stress tolerance. Plant Cell Environ 372:325–2338. https://doi.org/10.1111/pce.12422

Zhang C, Zhang Z, Zhang L, Li Q, Li C, Chen G, Zhang S, Liu Q, Hu X (2020) Evolution of the functionalities and structures of biochar in pyrolysis of poplar in a wide temperature range. Bioresour Technol 304:123003. https://doi.org/10.1016/j.biortech.2020.123002

Zhao C, Ma J, Li Z, Xia H, Liua H, Yang Y (2020) Highly enhanced adsorption performance of tetracycline antibiotics on KOH-activated biochar derived from reed plants. RSC Adv 10:5066. https://doi.org/10.1039/c9ra09208k